Fragmentation analysis of $^{88}Mo^{*}$ compound nucleus in view of different decay mechanisms

A thesis submitted in partial fulfillment of the requirements for the award of degree of

Master of Science

In

Physics

Submitted by

Bhaktima

(Roll No- 301704004)

Under the supervision of

Dr. Manoj K. Sharma

(Professor of Physics)

SPMS

School of Physics and Materials Science (SPMS)

Thapar Institute of Engineering and Technology,

Patiala-147004, INDIA

July- 2019

I dedicate this thesis to God and my loving family.

CERTIFICATE

I hereby certify that the work which has been presented in this dissertation entitled, "**Fragmentation analysis of ^{88}Mo compound nucleus in view of different decay mechanisms**" submitted in partial fulfillment of the requirements for the award of degree of **Master of Science** in **Physics** at **Thapar Institute of Engineering and Technology, Patiala,** is an authentic record of my own work carried out under the supervision of **Dr. Manoj K. Sharma, Professor, SPMS** and refers other researcher's work which are duly listed in reference section.

The matter embodied in this thesis has not been submitted for the award of any other degree of this or any other university.

Bhaktima

(Bhaktima)

Date: 15/07/2019

This is to certify that the above statement made by the candidate is correct and true to best of my knowledge.

15/7/19

Dr. Manoj K. Sharma

Professor

SPMS, TIET

Patiala

Acknowledgement

More so than anything else, I express my deepest thanks and gratitude to the All Powerful who has been there through it all.

It is of immense pleasure to acknowledge my sincere gratitude to **Dr. Manoj K. Sharma**, my worthy supervisor, **Professor of "School of Physics and Material Science."** Without him this dissertation would not have been viable. His guidance helped me in all the time of research and inscribing of this dissertation. His visionary thoughts have influenced me profoundly. It is of great pleasure to work under his supervision.

My sincere thanks also go to my mentor **Ms. Neha Grover**, research scholar, for the help and valuable suggestions provided by her. I got greatly benefited from her keen scientific insight and her knack for solving seemingly intractable difficulties. Her dedication, keen interest, kindness, scholarly advice and scientific approach have enabled me to complete my dissertation. I owe a debt of gratitude to all the members of the Nuclear Theory Lab for all the valuable guidance all through this effort.

Special thanks to my friends Ratika, Harpreet and Garima for all the joy that they brought into my life and the staff at the School of Physics and Material Science for providing me a friendly atmosphere and encouraging me round the slog.

I would like to express my heart-felt gratitude to my family for their love and support.

I also place on record, my sense of gratitude to one and all that directly or indirectly, have lent their hand in this venture.

Bhaktima

Date: 15/07/2019

Bhaktima

Contents

Page No.

List of figures

List of Tables:

Abstract

In order to study the decay dynamics associated with ^{48}Ti+ ^{40}Ca reaction, investigation are carried at three beam energies (E_{beam}=300,450 and 600 MeV) using Collective Clusterization approach of Dynamical Cluster Decay Model (DCM). Calculations are done for spherical and deformed choice of fragments having optimum orientations (θ_i^{opt}). According to the experimental evidence, ^{88}Mo* decays via Fusion-Evaporation (FE) and Fusion-Fission (FF) processes, thus the decay cross-sections of this hot and rotating compound system are calculated for both FE and FF channels.

This dissertation is focused on following three chapters.

Chapter-1:

Chapter-1 includes the basic introduction about nuclear reaction dynamics including its applications and benefits to mankind. In addition to this, various mathematical models dealing with reaction dynamics and related structural properties are briefly discussed here. Furthermore, nuclear reactions and their types on the basis of distinct parameters like energy, mass and compound nucleus formation etc. are enlightened. Besides this, a description of compound nucleus formation and its successive decay mechanisms is briefly outlined in view of dynamical evolution of heavy ion nuclear reactions at low energy regime.

Chapter-2:

Chapter-2 consists of the theoretical formalism used to understand reaction dynamics of ^{88}Mo* compound nucleus. The Dynamical Cluster-Decay Model (DCM) is used to analyze the fragmentation behavior for Fusion-Evaporation as well as Fusion-Fission decay processes.

Chapter-3:

Chapter-3 gives an account of the analysis of the Fusion-Evaporation and Fusion-Fission decay patterns of $^{88}Mo^{*}$ compound nucleus, within DCM framework. The results obtained & the conclusions drawn are duly discussed. Calculations are done over a wide range of incident beam energies and DCM based cross-sections are found in decent agreement with available experimental data.

CHAPTER: 1

Literature review of Nuclear Physics relevant to present work

CHAPTER:1

1.1 OVERVIEW:

The field of nuclear physics is very important pursuit as it expands our knowledge of both the infinitely small nucleons and the extremely large universe. This field mainly concerns itself with the structure and behaviour of the tiny inner core of an atom, which is termed as atomic nucleus. The study of atomic nuclei has historically given us many insight related to modern physics. Also, it is closely associated with various other branches of research such as particle physics, astrophysics, medical physics etc. Further, the atomic nucleus may exhibit both classical and quantum-mechanical behavior. In classical picture, it may behave like a liquid drop, whereas the quantum mechanical nature of the nucleus show shell structure similar to that found in atoms. The size of atomic nucleus is 10^5 times smaller than the atom, however it contains all the positive charge and essentially all the mass of the atom. The study of nuclear physics mainly aims to understand different forces responsible for the existence of nucleus and thus to understand different nuclear properties. Various theoretical models were developed to apprehend different nuclear forces and structural behavior of atomic nucleus.

Firstly, the classical picture of the nucleus and the basic dependence of binding energy on atomic mass number was explained by Liquid Drop Model (LDM). This model also provided the preliminary explanation of fission mechanism [1]. However, it failed to explain that high stability of some nuclei arises due to certain numbers of nucleons (proton and neutron) termed as “magic numbers”. Also, this model did not elucidate the measured spin and magnetic moments of nuclei. Thus, to overcome these issues, Maria Goeppert-Mayer and Hans Jensen developed shell model, which successfully explained the abundance and high stability of different nuclei with magic numbers. However, Shell model was unable to elaborate the deformations effects of nuclei, which were later explained by Nilsson model [2]. Later, the rotational and vibrational features were defined by Collective model. Further, to get more comprehensive picture of different nuclear properties, the Unified model depicting the combined characteristics of Shell model and collective model was deviced. Thus, by the formalism of all these nuclear models various nuclear properties and related structural effects were explained to interpret different nuclear phenomena. Thus,

these models were able to demonstrate different phenomena directed by the elementary forces (the gravitational force, electromagnetic force, weak force and strong force), which are accountable for all the phenomena occurring in the Universe. The gravitational forces are accountable for the existence of neuron stars (or gigantic nuclei). The electromagnetic force, weak force and strong forces play crucial role for the existence of an atomic nucleus, where the electromagnetic force is responsible for the charged particles (protons) interactions within the nucleus and weak forces give rise to the transformation between the nucleonic states. Further, the strong forces are capable to overcome the repulsive forces between densely packed protons in the nucleus and thus responsible for the nuclear survival.

The study of above mentioned nuclear forces is much essential to perceive the knowledge of different nuclear properties and behavior. Also, these forces play an important role in understanding the behavior of nuclear reactions [2]. Thus, the study of nuclear reactions is also very helpful to have a comprehensive knowledge of nuclear structure and related dynamics. A brief elucidation of nuclear reactions is given in the following section.

1.2 Nuclear Reactions:-

The study of nuclear reactions provides considerable information on the structure of the interacting nuclei as well as on the nature of their interaction. These reactions occur when two nuclei interact via strong forces and involve both kinematics and dynamics. In reaction kinematics, the general laws of energy and momentum conservation are duly considered via relativistic and non-relativistic motion. The reaction dynamics states different interaction mechanisms. The understanding of reaction dynamics is necessary to analyze various nuclear properties and related aspects at all possible extremities of energies, temperature, angular momentum and potentials such as angular momentum dependent potential, nuclear proximity potential, Coulomb potential etc. Depending upon different parameters such as beam energy (E_{beam}), projectile, mass of interacting nuclei and mechanism involved, nuclear reactions can be categorized in to various classes.

Depending upon beam energy range, nuclear reactions can be categorized into three forms as follows:

- **Low energy:** Low energy nuclear reactions deal with the basic properties, nuclear shape, size, reaction dynamics etc. with an energy range E≤ 15 MeV/nucleon.
- **Intermediate energy:** The analysis at this energy is mainly focussed on multi fragmentation, nuclear flow, particle production, balance energy etc. The energy range is in between 15 MeV/nucleon - 500 MeV/nucleon.
- **High energy:** At this energy regime, the main focus is to explore about the interactions between quark-gluon plasma and electromagnetic production of high energy particles such as leptons and mesons. The energy range is > 500 MeV/nucleon [3].

The above mentioned nuclear reactions have provided distinct requisite tools to understand dynamics and nuclear behavior comprehensively. The present dissertation work is mainly focused to the analysis of heavy ion reactions at low energy. Such reactions are constructively helpful to perceive detailed knowledge of nuclear structure and related dynamics. Description of Heavy Ion reactions (HIRs) is given in the forthcoming section.

1.3 Heavy Ion induced Reactions (HIRs) at low energies:-

The term 'heavy ion' is generally used for the nuclei which are heavier than the Helium nucleus. The availability of accelerators which can accelerate ions such as ^{12}C, ^{16}O, ^{40}Ar, ranging to Uranium or even beyond with incident energy 5 to 15 MeV per nucleon has opened a new field of nuclear physics termed as low energy HIRs. At low bombarding energies, Coulomb forces are more dominating, while the nuclear interaction play important role when the projectile energy is comparable to Coulomb barrier. For nuclear scientists, the study of heavy ion induced nuclear reactions is a matter of renaissance concern, as it provides the information to comprehend the basis of nuclear forces as well as the nuclear structures. In such reactions, the projectile and target may interact through three different ways: (i) The beam may deviate from its path due to the influence of target potential (ii) There might be the interaction of projectile and target either centrally or peripherally. (iii) The projectile may splits in to two or more fragments and one or more fragments may fuse with the target nucleus.

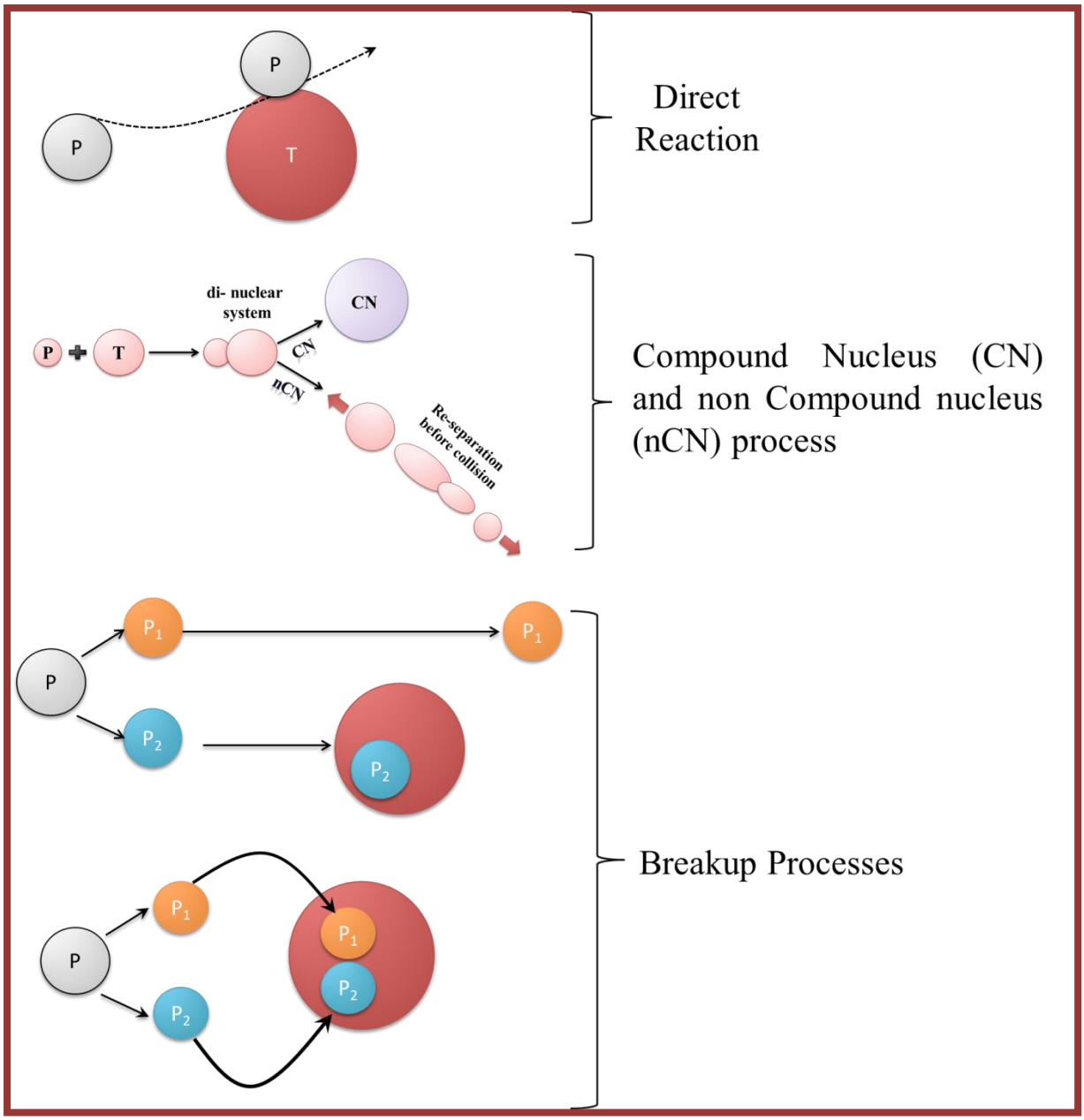

Fig. 1.1: *Pictorial representation of different reaction mechanisms [3].*

In first possibility, the feasible reaction mechanisms are direct reactions [4], where the projectile and target does not interact at all or interact through one or few nucleons. The main examples of direct reactions are stripping and pick up reactions. In the second possibility, projectile may amalgamate completely with the target nucleus and cause the emergence of equilibrated compound nucleus (CN) or interact partially with the target nucleus, which leads to the decay of composite system before achieving equilibrated CN configuration and the process is termed as non-compound nucleus (nCN) process. Finally, the third likelihood of HIRs states that the beam may break in to two or more fragments

and lead to Sequential Complete Fusion (SCF; all fragments fuse with target sequentially and form CN) or incomplete fusion (ICF; one of the fragments fuse with target and form CN) or Non-Capture Breakup (NCBU; no fragment fuse with the target) [5]. A pictorial representation of these possibilities is shown in Fig. 1. The present dissertation is mainly concerned with the compound nucleus reaction mechanisms occurring due to the complete amalgamation of projectile and target. The emergence and decay products of compound nucleus is described in the following section.

1.3.1 Compound Nucleus dynamics:-

Compound nucleus is one of the vital reaction mechanisms. Niel Bohr in 1936 proposed his theory of the compound nucleus for the interpretation of nuclear reactions. He assumed that most of the nuclear reactions involve two different stages.

(i) The incident particle strikes a "target nucleus" and the two form a compound nucleus having charge and mass numbers equivalent to the sum of charge and mass numbers of incident and target nucleus.
Incident Particle + target nucleus → Compound nucleus (CN)

(ii) The compound nucleus then disintegrates by emitting a product fragment such as neutron, proton, alpha particle or fission fragment.

The process mentioned in the first step is termed as **Complete Fusion (CF)**. In this process, the incident projectile is captured by the target nucleus and the energy of CN formed is shared or re-shared among its constituents until the memory of its mode of formation is lost, except that required by the conservation of energy, total angular momentum and parity. Further, the formed compound nucleus has a life time of the order of 10^{-16} - 10^{-14} sec. This life time may appear very short but it is sufficiently long as compared to the natural nuclear time i.e. (time taken by a nuclear particle with an energy of several MeV to pass through the nucleus), which is 10^{-22} - 10^{-21} sec. Bohr assumed that the mode of disintegration of compound nucleus depends upon its quantum mechanical properties such as excitation energy, parity and angular momentum. However, it is totally independent of its entrance channel properties because its life time is long enough to loose the memory of its formation [6]. Further, the compound nucleus may decay by emitting light particles (LPs), Intermediate Mass Fragments (IMFs), and Heavy Mass Fragments (HMFs) and fission fragments. Depending upon the mass of outgoing fragments, different decay modes are described below:

- **Evaporation Residue (ER)**

  Evaporation Residue forms a major decay channel for composite systems with the mass spread A≈50, where fission is usually negligible. The fragments emitted are basically the light particles like neutrons, protons, alpha particles ($A_2 \leq 4$ and $Z_2 \leq 2$) [7]. Also, for compound nuclei having mass A≈100-200, the intermediate and heavy mass fragments also starts contributing along with ER.

- **Intermediate and heavy mass fragments (IMFs and HMFs)**

  Intermediate mass fragments are also designated as clusters or complex fragments and the mass and charge range of IMFs is $5 \leq A \leq 20$; $2 \leq Z \leq 10$. Further, heavy mass fragments lie in between IMF and fission. Both IMF and HMF contributions are seen for compound systems having mass equivalent to A≈100-200. HMFs may also contribute in the decay of heavier compound nuclei (A ≥ 200), however with minor contribution [7-8].

- **Fission**

  Mass range of fission fragments generally equivalent to $\frac{A}{2} - 20 \leq A \leq \frac{A}{2} + 20$, where A is mass of compound systems. Fission is the dominant decay mode for compound nuclei having mass A ≥ 200, due to high Coulomb repulsion [8].

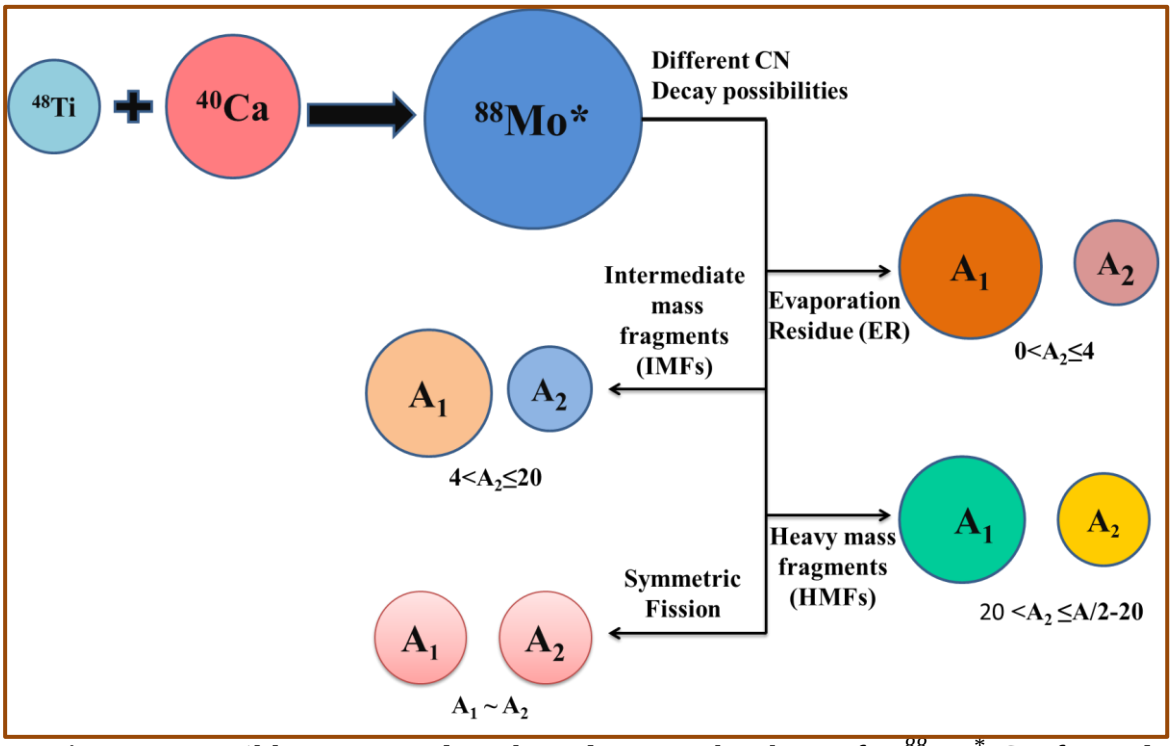

***Fig. 1.2**: Possible compound nucleus decay paths shown for $^{88}Mo^{*}$ CN formed in ^{48}Ti + ^{40}Ca reaction.*

Besides Compound nucleus decay mechanisms, there are some possible reaction mechanisms, where composite system decay before achieving the equilibrated configuration at compound nucleus stage. Such processes are termed as non-compound nucleus (nCN). Some of the nCN mechanisms are discussed below in Sec.1.3.2

1.3.2 Non-Compound Nucleus (nCN) Reactions:-

Depending upon the colliding partners, beam energy or mass asymmetry of interacting nuclei, there might be the possibility of some non-compound nucleus mechanisms, in which there is no formation of equilibrated compound nucleus. In such reactions there is an emergence of non-equilibrated composite system, which may decay through different nCN decay modes such as Deep inelastic Collision (DIC), Quasi Fission (QF) etc.

DIC mechanism is mainly noticed in the light mass region of composite systems (A≤80). The main features of this process are as follows:

- The projectile and the target nuclei interact peripherally for an adequate amount of time, which causes substantial dissipation of initial kinetic energy and angular momentum.
- It is generally observed for partially damped waves close to the grazing angle and the mass of the decay products is generally similar to the

projectile and target and thus termed as PLFs (Projectile Like Fragments) and TLFs (Target Like Fragments).

- The interaction potential pocket for DIC decay channel disappears, which implies that the composite system in this mechanism disintegrate without trapping in the pocket of interaction potential. Thus it is not governed by the full momentum transfer.

On the other hand, QF is the intermediate process between DIC and fission of the fully equilibrated compound nucleus. The primary features describing QF are as follows:

- The life time of the composite system formed in the QF process is comparatively larger than the one formed in DIC.
- It is predominantly influences by the entrance channel properties, viz. mass-asymmetry, deformation of colliding nuclei, collision energy and Coulomb factor Z_1Z_2.
- The QF contribution have been observed to increase with the increment in Coulomb factor Z_1Z_2 and behave as a dominant contributor for composite systems with $Z_1Z_2 > 1000$.

1.4 Role of Deformations:-

By following the idea of nuclear shape vibrations given by N. Bohr, the concept of the deformed nuclei was originated by "Pauli". He stated that the electromagnetic interactions of nucleons inside atomic nucleus are responsible for the hyperfine structure of energy levels (both atomic and molecular). Basically, the cause of non-spherical shape of atomic nuclei attributes to the shell effects i.e. if there is an addition or removal of few nucleons in magic nucleus (spherical), then there might exist the quadruple moment of new nucleus, which is signature of deformation. Further, the existence of deformation also signifies the symmetry breaking of nucleus. The study of shapes and deformations has always been the fascinating topic for nuclear physicist. One of the major reasons of this scrutiny is highly complex structure of the atomic nucleus and its relative properties. Till now, no such theory is established to elucidate the shape, structure and properties of nucleus completely. In this dissertation, the influence of quadruple deformations is explored for the decay of $^{88}Mo^{*}$ nucleus. The quadruple or β_2-deformations are modulated by the electric quadruple moment ($Q_0 = 2/5\ Z\ (b^2-a^2)$) with 'a' and

'b' as ellipsoid axis. The value of $Q_0=0$, $Q_0<0$, and $Q_0>0$ represent the spherical, oblate and prolate shapes of nuclei respectively [12]. Further, there is also possibility of higher order deformed shapes such as octupole (pear like shaped nuclei) and hexadecapole [13].

1.5 Nuclear Cross-sections:-

The nuclear reaction cross-section give a measure of the probability that an incident (bombarding) particle would interact in a certain way with the target nucleus. In order to understand this we have to visualize each target nucleus as presenting a certain area, called nuclear cross-section to the incident particles such that the incident particles striking within this area lead to nuclear reaction while the ones hitting outside this area do not induce nuclear reaction. Hence greater the cross-section greater is the likelihood of occurrence of reaction. The nuclear cross-section in general does not represent the geometrical cross-section of the target nucleus. In fact it may be greater than, equal to or less than the geometrical cross-section [$=\pi R^2$] of the target nucleus [16]. In this work, we have studied the evaporation residue and fission cross-sections for $^{88}Mo^*$ nucleus formed in $^{48}Ti + ^{40}Ca$ reaction.

1.6 Motivation:-

The study of different decay mechanisms of the compound nucleus (CN) had begun with the inception of modern nucleus physics and has maintained its peculiarity till now. The study of different decay modes of light and medium mass systems [17-21] has gained immense interest in recent times. Such outcomes have attributed significantly to the improvement of experimental techniques and refinement of theoretical formalisms. Several formalisms have been advanced to address different decay modes of the compound nuclei and thus to reconcile numerous issues related to the decay analysis.

In context of above, present work involves the decay analysis of $^{88}Mo^*$ nucleus formed in the $^{48}Ti + ^{40}Ca$ reaction. The decay of $^{88}Mo^*$ nucleus is investigated at three different beam energies (E_{beam}=300, 450, 600 MeV) by means of collective clusterization approach of the Dynamical Cluster Decay Model (DCM) [10, 23-26]. Calculations are done for both spherical and deformed choices of fragments. In accordance to ref. [22] $^{88}Mo^*$ decays through Fusion-Fission (FF) and Fusion- Evaporation (FE) decay paths, therefore the decay cross-sections of both FE as well as FF decay channels are estimated using

DCM framework. According to the experimental analysis [22], FF includes the Intermediate mass fragments (IMF), Heavy mass fragments (HMF) and fission fragments. Thus, the contribution of all three channels is included in FF decay cross-sections explicitly. Such analysis of fusion evaporation, IMF, HMF & fission will be of extreme importance to understand decay dynamics of light mass nuclei with A_{CN}<100.

References:

[1] Kenneth S. Krane**,** Introductory Nuclear Physics, Chapter **1**, Pg. No. 13.

[2]http://dspace.thapar.edu:8080/jspui/bitstream/10266/3779/1/Gurvinder_thesis_upload.pdf.

[3] D. C. Tayal, Nuclear Physics, Himalaya Publishing Group, Chapter **10**, Pg. No. 401.

[4] S. T. Butler, Phys. Rev. **80**, 1095 (1950); S. T. Butler, Proc. R. Soc. A **208**, 559 (1950); N. Austern, S. T.Butler, and H. Mcmanus, Phys. Rev. **92**, 350 (1953); J. R. Oppenheimer and M. Phillips, Phys. Rev. **48**, 500 (1935).

[5] N. Grover, K. Sandhu, M. K. Sharma, Nucl. Phys. A **974**, 56-71 (2018).

[6] S. N. Ghoshal, Phys. Rev.**80**, 6 (1950).

[7] M. Kumar, R. Kumar and M. K. Sharma, Phys. Rev. C **85**, 014609 (2012).

[8] N. Grover and M. K. Sharma, AIP Conference Proceedings 2006, 030007 (2018).

[9] N. Grover, Kanishka Sharma, and Manoj K. Sharma, Eur. Phys. J. A **53**: 239 (2017).

[10] N. Grover, G. Kaur, and M, K. Sharma, Phys. Rev. C **93**, 014603 (2016).

[11] P. M. Walker, F.R. Xu and D.M. Cullen, Phys. Rev. C **71**, 067303 (2005).

[12] R. Lucas, Europhysics News Vol. **32**, No. 1, 5-8, (2001).

[13] I. Maqbool, P. A. Ganai and J. A. Sheikh, Proceedings of the International Symposium on Nucl. Phys. **54**, 164 (2009).

[14] H. Sagawa, X. R. Zhou and X. Z. Zhang, Phys. Rev. C **72**, 054311 (2005).

[15] G. Kaur, D. Jain, R. Kumar, M. K. Sharma, Nucl. Phys. A **916**, 260274 (2013).

[16] A. Verma, P. Jain, and S. Kalia, Nuclear Physics book, S. Vikas & Co. (publishing house), Chapter **5**, Pg. No. 5/162.

[17] P. Roy, K. Banerjee, S. Bhattacharya, C. Bhattacharya *et al.*, Phys. Rev. C **86**, 044622 (2012).

[18] L. Morelli, G Baiocco, M D'Agostino, F. Gulminelli, *et al.*, J. Phys. G **41**, 075107 (2014).

[19] L. Morelli, G Baiocco, M D'Agostino, F Gulminelli, *et al.*, J. Phys. G **41**, 075108 (2014).

[20] A. Di Nitto, R. Moro1, A. Brondi, N. Gelli, *et al.*, EPJ Web Conf. **21**, 02002 (2012).

[21] A. Dey, S. Bhattacharya, C. Bhattacharya, K. Banerjee. *et al.*, Phys. Rev. C **74**, 044605 (2006).

[22] S. Valdré, S. Piantelli, G. Casini, *et al*. Phys. Rev. C **93**, 034617 (2016)

[23] R.K. Gupta, M. Balasubramaniam, R. Kumar, D. Singh, C. Beck and W. Greiner, Phys. Rev. C **71**, 014601 (2005).

[24] R. K. Gupta, M. Balasubramaniam, R. Kumar, D. Singh, S. K. Arun and W. Greiner, J. Phys. G: Nucl. Part. Phys. **32**, 345 (2006).

[25] M. Kaur, B. B. Singh, S. K. Patra, and R. K. Gupta, Phys. Rev. C **95**, 014611 (2017)

[26] G. Kaur, N. Grover, K. Sandhu, M. K. Sharma, Nucl. Phys. A **927**, 232-248 (2014).

CHAPTER: 2

Theoretical Formalism

CHAPTER:2

The Dynamical Cluster Decay Model (DCM)

Introduction:

The methodology used in the present work is termed as Dynamical Cluster Decay Model (DCM) [1-7]. This framework is basically reformulated version of Preformed Cluster Model (Methodology to study ground state emissions) [8-11] and is based on the well-established Quantum Mechanical Fragmentation Theory (QMFT) [12-13]. Also, it includes the effect of all essential components such as Temperature (T), excitation energy (E^*), angular momentum (ℓ), deformations (β) and orientations (θ).

Moreover, DCM has been applied to examine the decay paths and related structural aspects of numerous compound nuclei. Here I have implementing this framework to analyze the Fusion-Evaporation (FE) and Fusion-Fission (FF) decay channels of $^{88}Mo^*$ compound nucleus.

Essentially, DCM examines the decay process by using the following two-steps:

1. Firstly, it involves the calculation of preformation probability (P_o) of decay fragments, which are supposed pre-born in the compound nucleus prior to their tunneling across this potential barrier.
2. Secondly, it determines the barrier penetrability of the fragments using WKB method.

To pursue the first step or to study the binary fragmentation in DCM, the fragmentation potential is defined as follows:-

$$V(\eta, R, \ell, T) = -\sum_{i=1}^{2} B_i\left(A_i, Z_{i,}\beta_{\lambda i}, T\right) + V_c\left(R, Z_{i,}\beta_{\lambda i}, \theta_i, \phi, T\right) + V_p(R, A_i, \beta_{\lambda i}, \theta_i, \phi, T) \quad + V_\ell(R, A_i, \beta_{\lambda i}, \theta_i, \phi, T) \tag{1}$$

where the term B_i (i=1, 2) represents the binding energies of the two nuclei. Next, V_P, V_C, V_ℓ represent the T dependent Proximity, Coulomb and Centrifugal Potentials. These potentials are defined in the following subsections.

I. Proximity Potential (V_p) :

This potential comes in to nature when two interacting nuclei are at their close proximity distance. By using the appropriate values of mean curvature radius ($\bar{R}$(T)), Specific nuclear surface tension (γ), Surface width (b (T) =0.99(1+0.009T^2)), and Universal function $\phi(s_o,(T)$ (totally independent of structure and geometry), the expression of V_P [14] is given as:

$$V_P(s_o(T)) = 4\pi\bar{R}(T)\gamma b(T)\phi(s_o,(T)) \tag{2}$$

II. Coulomb Potential (V_c) :

Coulomb potential arising due to the charge of interacting nuclei can be written as: [15].

$$V_c(R, Z_i, \beta_{\lambda i}, \theta_i, T) = \frac{Z_1 Z_2 e^2}{R(T)} + 3Z_1 Z_2 e^2 \times \sum_{\lambda, i=1,2} \frac{R_i^{\lambda}(\alpha_i, T)}{(2\lambda+1)R(T)^{\lambda+1}} Y_{\lambda}^{(0)}(\theta_i)\left[\beta_{\lambda i} + \frac{4}{7}\beta_{\lambda i}^2 Y_{\lambda}^{(0)}(\theta_i)\right] \tag{3}$$

with $Y_{\lambda}^{(0)}(\theta_i)$ as the spherical harmonics function.

III. Centrifugal Potential (V_ℓ):

Centrifugal potential is based on angular momentum (ℓ) values of hot and rotating compound nucleus. The angular momentum is shifted from the entrance channel to the inner degrees of freedom of compound nucleus due to sliding friction between colliding partners [16]. The expression of V_ℓ is inscribed as:

$$V_\ell(T) = \frac{\hbar^2 \ell(\ell+1)}{2I(T)} \tag{4}$$

In the above Eqn. (4), I(T) represents the Moment Of Inertia (MOI) that has two limits non-sticking; [$I(T)=I_{NS}(T)= \mu R_a^2$] or sticking; [I(T)=$I_S$(T)=$\mu R_a^2+\frac{2}{5}mA_1R_1^2+\frac{2}{5}mA_2R_2^2$].

Present thesis work is pursued by incorporating I_S (sticking limit of MOI), in view of the use of proximity potential between two interacting fragments (R<2 fm).

Now the fragmentation potential with all its components work as an input in following time independent Schrödinger Equation in mass asymmetry η-coordinates.

$$\left\{-\frac{\hbar^2}{2\sqrt{B_{\eta\eta}}}\frac{\partial}{\partial\eta}\frac{1}{\sqrt{B_{\eta\eta}}}\frac{\partial}{\partial\eta}+V_R(\eta,T)\right\}\psi^{\nu}(\eta)=E^{\nu}\psi^{\nu}(\eta) \tag{5}$$

Here, in Eq. (5), ν signify ground (ν=0) and excited (ν=1,2,3…) vibrational states of compound nucleus. '$B_{\eta\eta}$' is the smooth classical hydro-dynamical mass parameter [17].

The solution of above equation with $V_R(\eta,T)$ (Eqn.10) as an essential input defines the Preformation probability, which is inscribed below.

$$P_0=\left(\frac{2}{A}\right)\sqrt{B_{\eta\eta}}\mid\Psi[\eta(A_i)]\mid^2 \tag{6}$$

ψ(η) represents the wave function and "A" represents the mass of compound nucleus.

After calculating Preformation probability, the next step is to determine the Barrier penetrability (P), using WKB method. The expression of penetrability read as

$$\mathrm{P}=\exp\left[-\frac{2}{\hbar}\int_{R_a}^{R_b}\{2\mu\left[V(R)-Q_{eff}\right]\}^{1/2}\,dR\right] \tag{7}$$

R_a is the first turning point and defined as:

$$R_a=R_t(\eta)+\Delta R=R_i(\alpha_i,T)+\Delta R(T) \tag{8}$$

In the above Eqn (8), ΔR specifies the neck between two interacting nuclei [18-19] or it is the relative separation between them.

$R_i(\alpha_i, T) = R_{0i}(T)[1 + \sum_{\lambda i} Y_\lambda^{(0)}(\alpha_i)]$ is radius vector, which comprehend the neck emergence and deformations of two interacting nuclei at their closest proximity distance. Further, the dependence of temperature in radii R_{0i} [20] is defined as:

$$R_{0i} = [1.28A_i^{1/3} - 0.76 + 0.8A_i^{-1/3}](1 + 0.0007T^2) \quad (9)$$

Further, the effective Q-value (Q_{eff}) in eqn. (7) is given as follows:

$$Q_{eff}(T) = B(T) - [B_1(T = 0) + B_2(T = 0)] \quad (10)$$

$$= \text{TKE (T) (Total Kinetic energy)}$$

$$= V(R_a) \text{ (Scattering Potential at } R_a)$$

After determining Preformation probability (P_o) & Penetrability (P), the decay cross-section in DCM are estimated by using Partial wave analysis as follows:

$$\sigma = \frac{\pi}{k^2} \sum_{l=0}^{l_{max}} (2l + 1) P_0 P \quad (11)$$

Where $k = \sqrt{\frac{2\mu E_{c.m.}}{\hbar^2}}$ is wave number, in which $\mu = \left[\frac{A_1 A_2}{(A_1 + A_2)}\right] m = \frac{1}{4} Am(1 - \eta^2)$ is reduced mass. $E_{c.m.}$ is center of mass energy and is given as $E_{c.m.} = E_{CN}^* - Q$ (with excitation energy, $E_{CN}^* = \left(\frac{A}{9}\right) T^2 - T$). Further, ℓ_{max}, in Eq. (11) signifies the maximum angular momentum which is set for vanishing the fusion barrier of the entrance channel η_i or where the light particle cross-sections become infinitely small ($\sigma_{LP} \rightarrow 0$).

By using the above mentioned methodology, the present work is aim to demonstrate the decay analysis of $^{88}Mo^*$ nucleus formed in $^{48}Ti + ^{40}Ca$ reaction in reference to the recent experimental data [21]. The details of calculations, observations drawn along with conclusions and brief outcome of the work are described in next chapter.

References:

[1] R. K. Gupta, M. Balasubramaniam, R. Kumar, D. Singh, C. Beck and W. Greiner, Phys. Rev. C **71**, 014601 (2005).

[2] R. K. Gupta, M. Balasubramaniam, R. Kumar, D. Singh, S. K. Arun and W. Greiner, J. Phys. G: Nucl. Part. Phys. **32**, 345 (2006).

[3] M. Kaur, B. B. Singh, S. K. Patra, and R. K. Gupta, Phys. Rev. C **95**, 014611 (2017)

[4] N. Grover, G. Kaur, and M. K. Sharma, Phys. Rev. C **93**, 014603 (2016)

[5] G. Kaur, N. Grover, K. Sandhu, M. K. Sharma, Nucl. Phys. A **927**, 232-248 (2014).

[6] N. Grover, I. Sharma, G. Kaur, M. K. Sharma, Nucl. Phys. A **959**, 10-26 (2017).

[7] S. Kumar and R. K. Gupta, Phys. Rev. C **55**, 218 (1997).

[8] R. Kumar, K. Sandhu, M. K. Sharma, and R. K. Gupta, Phys. Rev. C **87**, 054610 (2013).

[9] R. Kumar and M. K. Sharma, Phys. Rev. C **85**, 054612 (2012).

[10] G. Sawhney, M. K. Sharma and R. K. Gupta, Phys. Rev. C **83**, 064610 (2011).

[11] S. Kumar and R. K. Gupta, Phys. Rev. C **55**, 054612 (2012).

[12] J. Maruhn and W. Greiner, Phys. Rev. Lett. **32**, 548 (1974).

[13] R. K. Gupta, W. Scheid, and W. Greiner, Phys. Rev. Lett. **35**, 353 (1975).

[14] J. Blocki, J. Randrup, W. J. Swiatecki, and C. F. Tsang, Ann. Phys. (NY) 105, 427 (1977).

[15] N. Grover, K. Sandhu, Manoj K.Sharma, Nucl. Phys. A **974,** 56–71 (2018).

[16] P. Glässel, R. S. Simon, R. M. Diamond, R. C. Jared, *et al.*, **38**, 331 (1977).

[17] H. Kroger and W. Scheid, J. Phys. G Nucl. Phys. **6**, L 85 (1980).

[18] S. Kumar and R. K. Gupta, Phys. Rev. C **55**, 218 (1997).

[19] R. K. Gupta, S. Kumar, and W. Scheid, Int. J. Mod. Phys. E **6**, 259 (1997).

[20] G. Royer and J. Migner, J. Phy. G **18**, 1781 (1992), and earlier references therein.

[21] S. Valdré, S. Piantelli, G. Casini, et al. Phys. Rev. C **93**, 034617 (2016).

CHAPTER: 3

Theoretical Observations & Calculations

CHAPTER:3

3.1 Introduction:

The quest of different nuclear structure properties and related dynamics has always been an interesting and challenging topic for both experimental and theoretical nuclear physicists. Heavy ion Fusion-Fission reactions have proved to be immensely helpful for this purpose or to understand the exotic nature of different nuclei. Presently, the decay of different compound nuclei formed in variety of Heavy Ion Induced Reactions (HIRs) has become a compelling subject [1-6], since it is able to produce new isotopes that do not occur naturally. Moreover, such mechanisms also provide comprehensive knowledge of numerous nuclear properties and related structive and dynamical effects.

In view of this, the dissertation is primarily focused on the decay analysis of compound nucleus ($^{88}Mo^{*}$) formed in $^{48}Ti + ^{40}Ca$ reaction. Decay analysis of the above mentioned compound nucleus is made using the Dynamical Cluster Decay Model (DCM) [7-12] in context to the recent experimental data [13]. Calculations are done at three beam energies (E_{beam}=300, 450, 600 MeV) by opting both spherical and β_2-deformed configuration of decaying fragments. In this work, cross-sections of both Fusion- Evaporation (FE) and Fusion-Fission (FF) decay channels are estimated for $^{48}Ti + ^{40}Ca \rightarrow ^{88}Mo^{*} \rightarrow A_1 + A_2$ reaction, where A_1 and A_2 respectively represent the heavy and light mass fragments in outgoing channel. Results and discussions are presented in the next Section 3.2.

3.2 Results and Discussions:

This section presents the details of calculations for the decay analysis of $^{88}Mo^{*}$ nucleus using the DCM framework. Further, the influence of different components such as incident energy, angular momentum (ℓ), deformations (β) on the variation of fragmentation potential (V_η), mass distribution, penetrability and decay cross-sections is discussed for the chosen compound nucleus. To explain the results explicitly, this section is segregated in to two parts, where Sec. 3.2.1 depicts the analysis for Fusion-Evaporation (FE) channel of $^{88}Mo^{*}$ and Fusion-Fission (FF) path is discussed in Sec. 3.2.2. Finally the results are summarized in section 3.3.

3.2.1 Fusion evaporation (FE) analysis of $^{88}Mo^{*}$

In this section, the main focus is to study the likelihood of the emission of light particles in decay of $^{88}Mo^{*}$ nucleus. To pursue the same, firstly, the fragmentation potential at optimized neck length parameter (ΔR) (See Eq. (8) of chapter 2) for Evaporation residue is plotted at two extreme angular momentum values in Fig. 3.1.

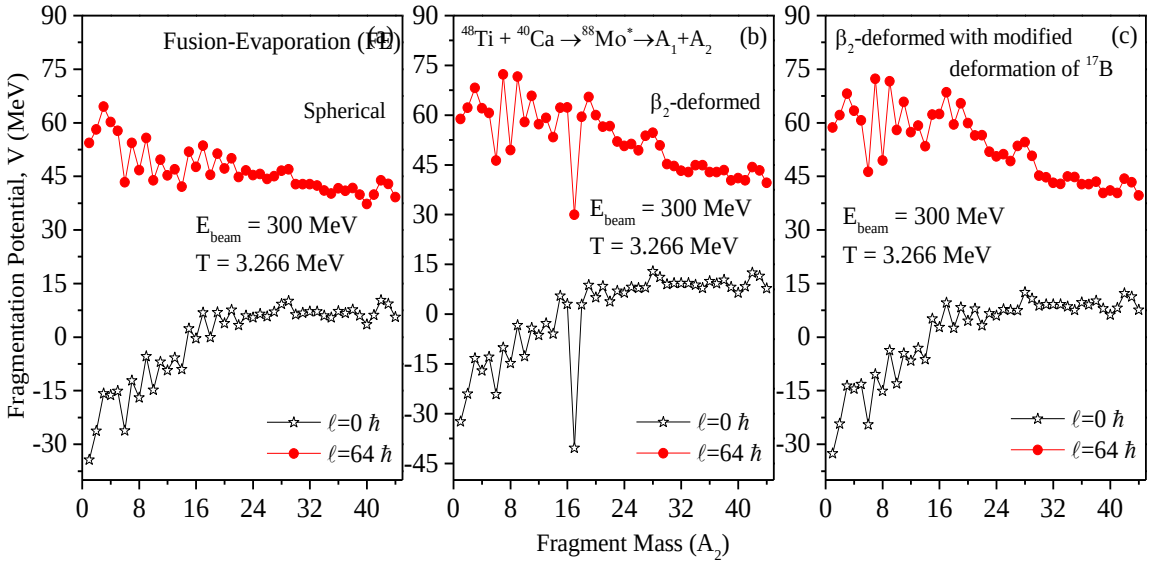

Fig. 3.1: *The behavior of Fragmentation potential with respect to the fragment mass for $^{48}Ti+^{40}Ca\rightarrow\ ^{88}Mo^{*}$ reaction at extreme ℓ value (ℓ =0&64) for the spherical and β_2-deformed fragments in exit channel.*

This figure depicts the variation of $V_R(\eta)$ at E_{beam}=300 MeV as a function of fragment mass for both spherical and β_2 deformed choice of fragments at corresponding optimum orientation (θ^{opt}) criteria. Here, it is worth mentioning that the fragments having minima in $V_R(\eta)$ are the most probable candidates in exit channel as they require lesser potential to penetrate the barrier. It is clearly evident from the Fig.3.1 that the emission of light particles is dominant at ℓ=0ħ for both spherical and deformed choices of fragments. However, with the increase in ℓ-values, the value of $V_R(\eta)$ for fission region start comparing with ER channel which signify the prominence of fission fragments at maximum angular momentum. In other words, Fusion Fission (FF) starts operating at the cost of FE at higher ℓ-values. Further, moving towards the influence of deformations, it may be noticed from the Fig. 3.1 (b) that there is sharp minima at ^{17}B for deformed choice of fragments. Interestingly, similar results were observed for the decay of $^{96}Tc^{*}$ nucleus in ref. [10], which state that this abrupt

minima at ^{17}B might be due to its inappropriate β_2-deformation. It is relevant to note that β_2-deformations are taken from Moller and Nix [14] where certain values are obtained after interpolations and extrapolations and hence there exists a possibility that β_2-values of certain fragments may not be accurate. Thus to rectify this problem, modified β_2-deformation of ^{17}B is used from [12], and the results are presented in Fig. 3.1(c), which show the expected behavior of fragmentation potential. As a result, further calculations are made using modified β_2-deformation for ^{17}B fragment (i.e β_2= 0.620). Similar results are obtained at maximum energy, E_{beam}=600 MeV (not shown here to avoid repetition).

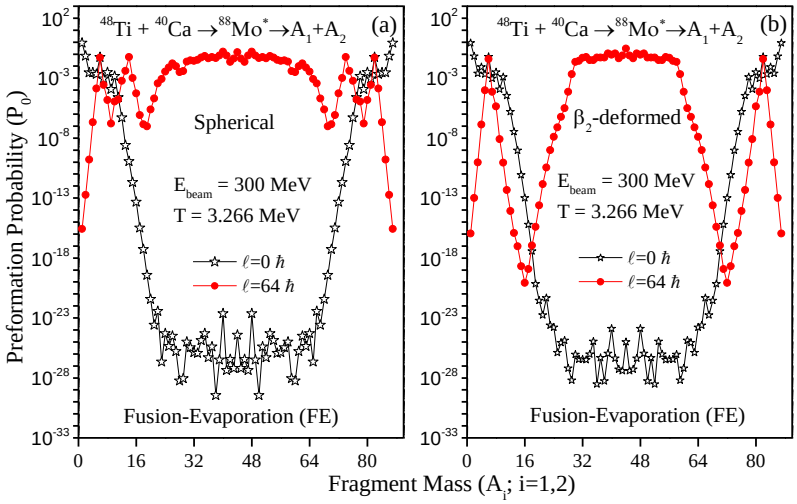

Fig. 3.2*: The variation of Preformation Probability (P_o) as a function of fragment mass at extreme ℓ-values for (a) spherical and (b) β_2-deformed choice of fragments obtained using the optimize neck value for Fusion-evaporation channel.*

As explained in Chapter 2, the fragmentation potential works as an essential input in Schrodinger wave Equation (Eq.(5) of Chapter 2), solution of which defines the preformation probability (P_0) of fragments which in turn participate in the exit channel. This preformation factor confers significant structural information of compound nucleus that otherwise does not exist in competing statistical models. Here, the preformation probability of ^{88}Mo* nucleus is displayed in Fig. 3.2 at E_{beam}=300 MeV. It is clearly evident from the figure that P_0-factor of light particles is much higher at ℓ=0ħ, however at $\ell = \ell_{max}$ fission starts competing. This observation is similar to the one perceived from Fig. 3.1 where the fragmentation potential is plotted as a function of fragment mass.

Next, to see the effect of angular momentum (ℓ) and energy, the summed up preformation probability is plotted as a function of angular momentum at three incident energies in Fig. 3.3. This figure clearly reveals that the $\sum P_0$ decreases with increase in energy, which implies that the decay cross-sections of light particles should be maximum at lowest energy. This observation is in line with the observation of [7]. Next, if one observe the influence of angular momentum on $\sum P_0$ of light particles, it is clearly visible from the Fig. 3.3 that the values of $\sum P_0$ are higher at lower ℓ values and there is steep fall in its magnitude with increment in ℓ. Further, it can also be noticed from the Figs. 3.3(a) and (b) that effect of energy and angular momentum does not change with the inclusion of deformation effects.

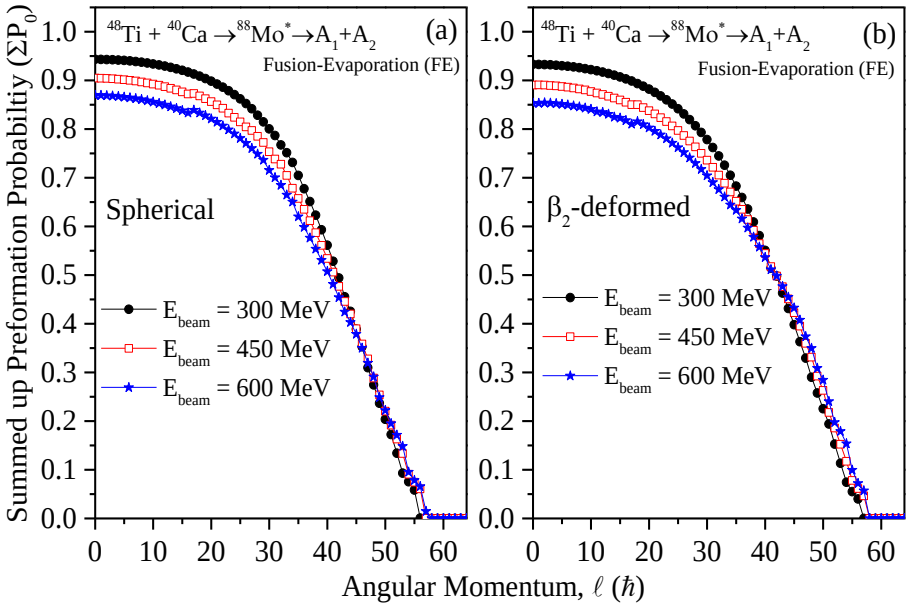

***Fig. 3.3**: Summed up Preformation Probability ($\sum P_o$) as a function of angular momentum for Fusion-Evaporation (FE) channel at beam energies (E_{beam}=300,450 and 600MeV.)*

After getting the information related to fragmentation potential and preformation probability, it is important to understand the tunneling probability of decay fragments as it contributes in the assessment of decay cross-sections. For this, the barrier modification (ΔV_B) and the tunneling probability/ penetrability (P) is analyzed for the most probable light fragment in Fig. 3.4. This figure demonstrate the behavior of ΔV_B (panel-a) and penetrability (panel-

b) as a function of angular momentum. One may clearly notice from the Fig. 3.4(a) that, the magnitude of ΔV_B is higher at lower ℓ-values and decreases with the rise in angular momentum. This signify that to tunnel the barrier at higher angular momentum, the required barrier modification is less in comparison to that at lower ℓ-values. As a consequence, the penetrability also increases with the increment in angular momentum, as evident from Fig. 3.4(b).

After estimating the Preformation probability and penetrability, the Fusion-Evaporation (FE) decay cross-sections are calculated and the results are displayed in Table 3.1 along with the respective components such as center of mass energy ($E_{c.m.}$), Temperature (T), maximum angular momentum (ℓ_{max}), and optimized neck parameter (ΔR). Also, it is clearly visible from the table that FE decay cross-sections are in reasonable agreement with the available data for both spherical and deformed choice of nuclei.

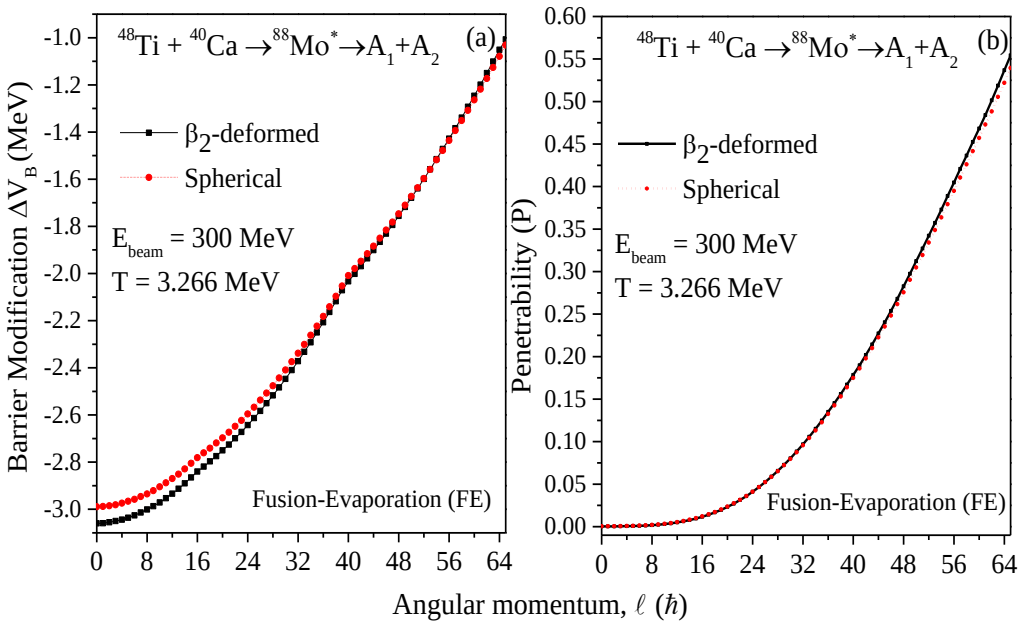

***Fig. 3.4**: The variation of (a) barrier modification (ΔV_B) and (b) Penetrability, P as a function of angular momentum (l) for Fusion-Evaporation channel at E_{beam}=300MeV.*

***Table 3.1**: Fusion-Evaporation (FE) cross-sections for $^{48}Ti + {}^{40}Ca \rightarrow {}^{88}Mo^*$ reaction at three given beam energies calculated using DCM and compared with the experiment data [7].*

E_{lab} (MeV)	$E_{c.m.}$ (MeV)	Temp. (MeV)	Spherical			Deformed			σ_{exp} (mb)
			ΔR (fm)	ℓ_{max} ($\hbar$)	σ_{DCM} (mb)	ΔR (fm)	ℓ_{max} ($\hbar$)	σ_{DCM} (mb)	
300	136.36	3.266	1.86	64	848	1.85	64	859	893±109
450	204.545	4.048	2.00	64	569	1.95	64	521	545±45
600	272.727	4.701	2.18	64	475	2.10	64	412	459±115

Now, the analysis of Fusion-Fission (FF) fragments is presented in the forthcoming section 3.2.2.

3.2.2 Fusion-Fission (FF) analysis of $^{88}Mo^*$ nucleus.

In this section, the main focus is to analyse the decay characteristics of FF fragments. Experimentally [13], it has been observed that FF fragments may involve symmetric fission fragments, near symmetric fragments (nSF), Intermediate Mass Fragments (IMFs) and Heavy Mass Fragments (HMFs). Thus, the analysis of all mass regions of FF is discussed in this section.

Firstly, the fragmentation potential (V_R (η)) as a function of fragment mass at E_{beam}=300 MeV is displayed in Fig. 3.5 by using the optimize neck parameter of FF. It is clearly depicted in Fig. 3.5 that at ℓ=0ħ, the fragmentation potential of fusion-fission fragments is higher than that of the FE fragments, however at ℓ= ℓ_{max}, FF region require less V_R (η) in the decay channel. This implies that FF fragments are more dominant at higher ℓ-values. To justify this observation, the preformation probability for the same is plotted in Fig. 3.6 for both spherical (panel-a) and deformed (panel-b) choice of fragments.

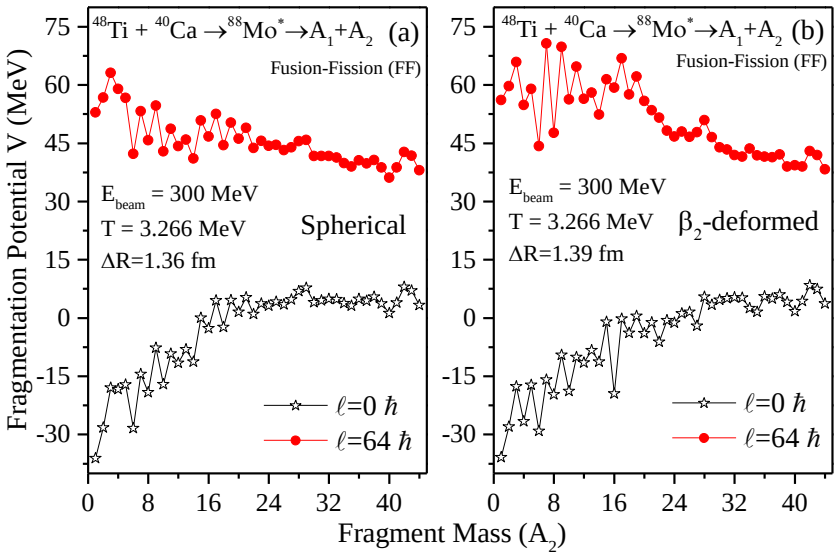

Fig. 3.5: *The Fragmentation potential as a function of fragment mass for the decay of* $^{88}Mo^{*}$ *nucleus at extreme ℓ-values obtained using optimized neck values for FF decay channel for spherical & deformed choices of decay fragments.*

Fig.3.6 clearly states that fission fragments are more probable at higher angular momentum, which is also in agreement with the available experimental systematics [7]. Further, one can also observe the role of deformations from Fig. 3.6, which exhibit that for spherical case, fission fragments cover relatively wide range ($A_{fission}$=26-62) in comparison to that for the deformed case. The IMFs and HMFs are peaked around A_{IMF}= 5-15 and A_{HMF}=21-25 respectively. However, after including the deformations, asymmetric peak at (A_2=6) start appearing with complementary heavy fragment (A_2=82), it is also evident from the Fig 3.6 that for deformed case the fission fragments cover mass range equal to ($A_{fission}$=29-59) and HMFs become relatively less prominent. Similar results are obtained at higher energy, E_{beam} = 600 MeV (not shown here to avoid repetition).

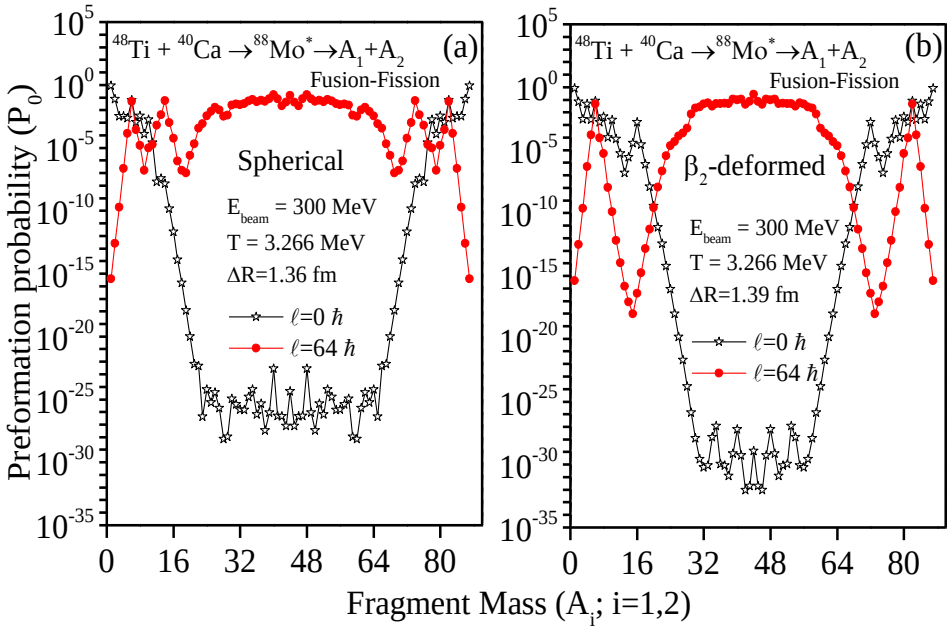

Fig. 3.6: *The Preformation probability (P_o) as function of fragment mass for the decay of $^{88}Mo^*$ nucleus at extreme ℓ-values obtained using optimized neck values for FF decay channel for spherical & deformed choices of fragments.*

Finally, the FF cross-sections for $^{88}Mo^*$ nucleus are tabulated in Table 3.2. Also, the Temperature (T), centre of mass energy ($E_{c.m.}$), maximum ℓ-value and optimized neck values are mentioned in Table 3.2. The calculated cross-sections find reasonable agreement with experimental data except at highest energy E_{lab}=600MeV.

Table 3.2: *Fusion-Fission (FF) cross-sections for ^{48}Ti + ^{40}Ca → ^{88}Mo* reaction at three given beam energies calculated using DCM and compared with the experiment data [7].*

E_{lab} (MeV)	$E_{c.m.}$ (MeV)	Temp. (MeV)	Spherical			Deformed			Σ_{exp} (mb)
			ΔR (fm)	ℓ_{max} ($\hbar$)	σ_{DCM} (mb)	ΔR (fm)	ℓ_{max} ($\hbar$)	σ_{DCM} (mb)	
300	136.36	3.266	1.36	64	121	1.39	64	111	115±3
450	204.545	4.048	1.62	64	245	1.67	64	261	266±37
600	272.727	4.701	1.89	64	383	1.94	64	388	459±115

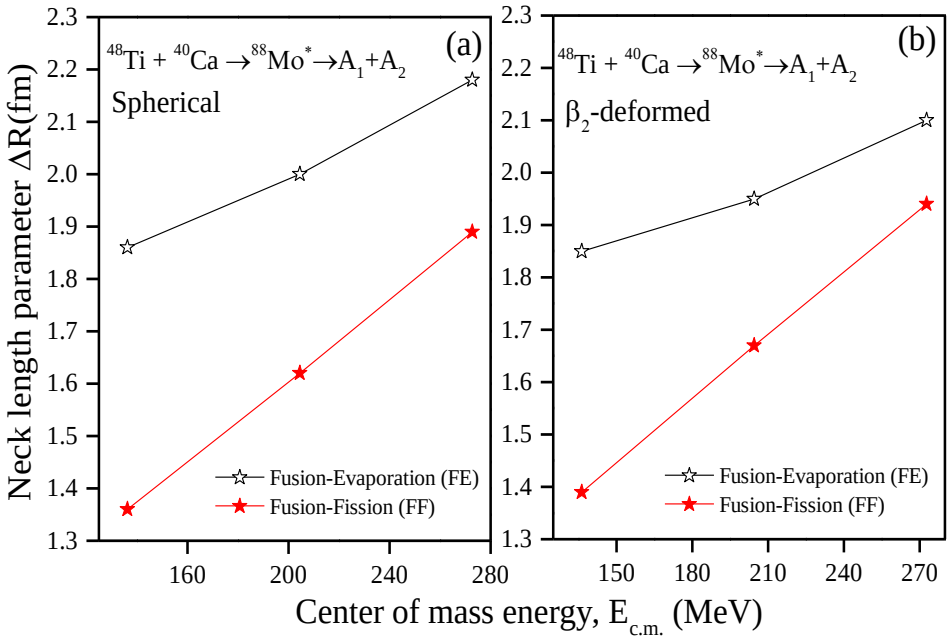

***Fig. 3.7**: Optimized neck length parameter (ΔR) of Fusion Evaporation & Fusion Fission channel as a function of centre of mass energy $E_{c.m.}$ for both spherical and deformed cases.*

After analysing the Fusion evaporation and Fusion fission separately, a comparative analysis of both is presented in terms of their neck value (ΔR) and decay cross-sections as a function of centre of mass energy in Fig. 3.7 and Fig 3.8 respectively. Fig. 3.7 demonstrates the variation of neck parameter for FE and FF by considering spherical and deformed choices of decay fragments. It is visible from the figure that higher neck value is required to emit light particles from ^{88}Mo* nucleus for both the cases (Spherical and β_2-deformed). Also, the incorporation of ΔR in DCM can directly be linked with the barrier modification (in-built property of DCM). It has been observed [13] that the lower neck value corresponds to the higher barrier modification, thus in the decay of ^{88}Mo* nucleus the fission fragments will require higher barrier modification in comparison to that of the Fusion evaporation process.

Fig. 3.8 displays the variation of FE and FF decay cross-sections compared with corresponding experimental data. This figure illustrates that the fusion evaporation cross-section decreases with the increase in energy, however fusion-fission cross-sections increases with rise in energy. Here, it is worth to mention that both type of cross-sections (FE and FF) addressed using DCM lie within the experimental error bars for both spherical and β_2-deformed choices of nuclei.

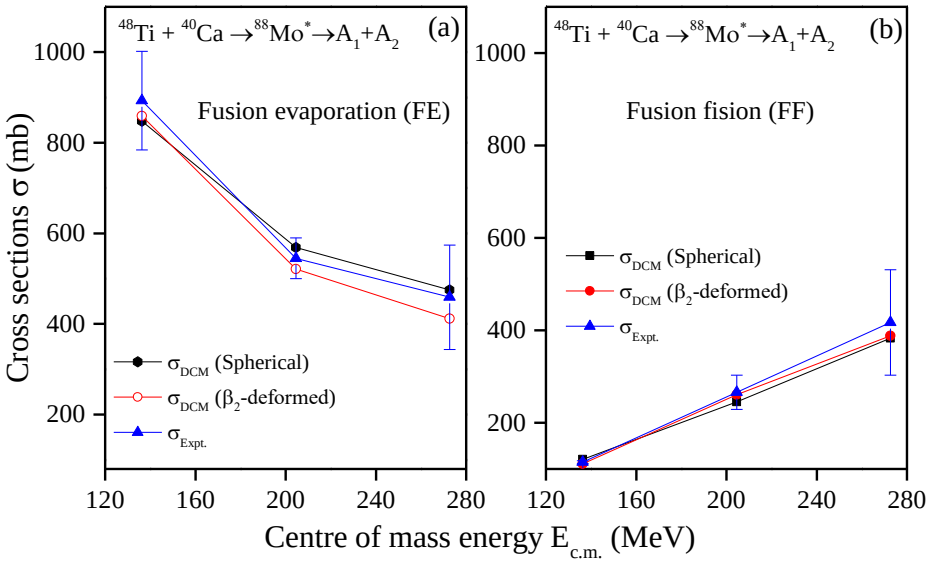

Fig. 3.8*: The variation of DCM calculated Fusion evaporation(FE) and Fusion fission(FF) cross-sections with respect to the centre of mass energy for spherical and deformed choice of fragments at three incident beam energies E_{lab}=300,450 and 600 MeV compared with the experimental data [7].*

References:

[1] S. J. Sanders, D.G. Kovar, B.B. Back, C. Beck, et al, Phys. Rev. C **40**, 2091 (1989).

[2] S. J. Sanders, B.B. Back, R.V.F. Janssens, D.G. Kovar, et al, Phys. Rev. C **41**, R1901 (1990).

[3] S. J. Sanders, A. Szanto de Toledo, C. Beck, Phys. Rep. **311**, 487 (1999).

[4] B. B. Back, H. Esbensen, C. L. Jiang, K. E. Rehm, Rev. Mod. Phys. **86**, 317 (2014).

[5] L. F. Canto, P. R. S. Gomes, R. Donangeloa, J. Lubianb, M. S. Hussein, Phys. Rep. **596**, 1 (2015).

[6] J. J. Kolata, V. Guimaraes, E.F. Aguilera, Eur. Phys. J. A **52**, 123 (2016).

[7] R. K. Gupta, M. Balasubramaniam, R. Kumar, D. Singh, C. Beck and W. Greiner, Phys. Rev. C **71**, 014601 (2005).

[8] R. K. Gupta, M. Balasubramaniam, R. Kumar, D. Singh, S. K. Arun and W. Greiner, J. Phys. G: Nucl. Part. Phys. **32**, 345 (2006).

[9] M. Kaur, B. B. Singh, S. K. Patra, and R. K. Gupta, Phys. Rev. C **95**, 014611 (2017)

[10] G. Kaur, N. Grover, K. Sandhu, M. K. Sharma, Nucl. Phys. A **927,** 232(2014).

[11] P. Arumugam, B. K. Sharma, and S. K. Patra, Phys. Rev. C **71,** 064308 (2005).

[12] G. Kaur, D. Jain, R. Kumar, M. K.Sharma, Nucl. Phys. A **916,** 260–274 (2013).

[13] S. Valdré, S. Piantelli, G. Casini, S. Barlini, *et al*, Phys. Rev. C **93**, 034617 (2016)

[14] P. Möller, J. R. Nix, W. D. Myers, and W. J. Swiatecki, At. Nucl. Data Tables 59,185 (1995).

Summary:-

This dissertation is primarily focused on the decay analysis of compound nucleus (CN) ($^{88}Mo^{*}$) formed in ^{48}Ti + ^{40}Ca reaction. Decay analysis of the above mentioned compound nucleus is made using the Dynamical Cluster Decay Model (DCM) in context to the recent experimental data. Calculations are done at three beam energies (E_{beam}=300, 450 and 600MeV) by opting two configurations of nuclei spherical and deformed. The cross-sections for Fusion-Evaporation (FE) and Fusion-Fission (FF) decay channels are estimated for $^{48}Ti+^{40}Ca \rightarrow {}^{88}Mo^{*} \rightarrow A_1+A_2$ reaction where A_1 and A_2 represent the outgoing fragments.

Firstly, the variation of Fragmentation potential and Preformation probability for FE channel states that the emission of light particles is more dominated at lower l-values, however at higher angular momentum values, fission start competing. Also, the contribution of FE cross-section is maximum at lower energy and start decreasing with rise in incident energy. Whereas, the FF contribution increases with the increment in energy. Further, moving towards the role of deformations, it has been observed that the fission fragments cover relatively wide range ($A_{fission}$=26-62) for spherical consideration in comparison to that for deformed case. The IMFs and HMFs are peaked around A_{IMF}= 5-15 and A_{HMF}=21-25 respectively. After including the deformations, asymmetric peak at (A_2=6) start appearing with complementary heavy fragment (A_2=82).

Finally, the decay cross-sections of both decay channels (FE & FF) are addressed using Dynamical Cluster Decay Model, which are in reasonable agreement with the available experimental data. It is important to mention that the above mention work can be extended further, as $^{88}Mo^{*}$ may also decay through nCN decay channel such as Deep Inelastic orbiting. Thus, it would be of future interest to exercise the possible emergence of DIC channel for this nucleus in framework of DCM approach.

Submission ID: 1150385400

Bhaktima Thakur MSc Thesis V03

ORIGINALITY REPORT

9%	2%	5%	8%
SIMILARITY INDEX	INTERNET SOURCES	PUBLICATIONS	STUDENT PAPERS

PRIMARY SOURCES

1	Submitted to Thapar University, Patiala Student Paper	6%
2	rnumata.org Internet Source	<1%
3	Jain, Deepika, Raj Kumar, and Manoj K. Sharma. "Reaction dynamics of Pt^{*} isotopes formed using stable and radioactive Sn beams", Physical Review C, 2013. Publication	<1%
4	Neha Grover, Kanishka Sharma, Manoj K. Sharma. "Dynamics of 47V* formed in 20Ne + 27Al reaction in view of fusion-fission and DIC mechanism", The European Physical Journal A, 2017 Publication	<1%
5	G. Sawhney, M. K. Sharma. "Dynamical decay process of 219, 220Ra* formed in 10, 11B + 209Bi reactions", The European Physical Journal A, 2012 Publication	<1%